

# Vapor–Liquid Equilibrium for the Difluoromethane (R32) + *n*-Butane (R600) System

Laura Fedele,<sup>\*,†</sup> Sergio Bobbo,<sup>†</sup> Mauro Scattolini,<sup>†</sup> Roberto Camporese,<sup>†</sup> and Roman Stryjek<sup>‡</sup>

National Research Council, Institute of Building Technologies – Division of Padova, Corso Stati Uniti 4, I-35127 Padova, Italy, and Institute of Physical Chemistry, Polish Academy of Sciences, Kasprzaka 44/52, 01-224 Warsaw, Poland

Vapor–liquid equilibria (VLE) for the difluoromethane (R32) + *n*-butane (R600) system that shows liquid-phase immiscibility below 246 K were measured at (263.15, 278.15, and 293.15) K by means of a static analytical method. The ( $T$ – $P$ – $x$ – $y$ ) VLE data were correlated using various equations of state and various mixing rules to compare the ability of these models to correlate data for this strongly nonideal system. The correlation of the VLE data and published VLLE data shows that the system is azeotropic at temperatures higher than the upper critical end point, UCEP, (246 K), heterohomoazeotropic between (246 and 230) K, and heteroazeotropic below 230 K. A comparison with the available VLE data in the literature was performed.

## Introduction

Mixtures formed by hydrocarbons and hydrofluorocarbons are promising substitutes for chlorinated refrigerants. Continuing our studies on liquid–liquid equilibria (LLE) of difluoromethane (R32) + *n*-butane (R600)<sup>1</sup>, R32 + propane (R290),<sup>2</sup> and pentafluoroethane (R125) + R600<sup>3</sup> systems and on vapor–liquid equilibria (VLE) of R32 + R290<sup>4</sup> and R125 + R600<sup>5</sup> systems, we measured the ( $P$ – $T$ – $x$ – $y$ ) VLE data for the R32 + R600 system at (263.15, 278.15, and 293.15) K. The system is strongly nonideal and forms a positive azeotrope within the experimental temperature range, but it shows liquid-phase splitting<sup>1</sup> below 246 K.

Various equations of state and mixing rules were used to correlate the data to compare their ability to describe this system. In addition, a comparison between our results and the recently published data of Shimawaki and Fujii<sup>6</sup> was made by using the same model.

## Experimental Section

**Chemicals.** R32 (difluoromethane, CH<sub>2</sub>F<sub>2</sub>) was supplied by Ausimont with a declared purity of >99.99%, and R600 (*n*-butane, C<sub>4</sub>H<sub>10</sub>) was supplied by Aldrich with a stated purity of >99%. After the elimination of the noncondensable gases, we detected no impurities by gas chromatographic analysis with either a thermal conductivity (TCD) or a flame ionization detector (FID); a Porapak Q column with a length of 2 m and an external diameter of 1/8 in. was used. All samples were used with no further purification.

**Apparatus.** The employed VLE experimental apparatus has been described.<sup>7</sup> Its main part is the stainless steel equilibrium cell of about 50-cm<sup>3</sup> capacity, equipped with two glass windows to allow the visual observation of the mixture. A magnetic pump was used to recirculate the vapor through the liquid to get faster equilibrium of the

sample in the cell. The VLE cell and the magnetic pump were immersed in a thermostatic water and ethylene glycol bath of about 100-L capacity whose temperature was controlled by means of a PID-controlled system governing a heater immersed in the bath. An auxiliary thermostatic bath was used to compensate for the heat produced by the PID-controlled system. The temperature in the bath was stabilized at  $\pm 1$  mK throughout the measurements. Temperature was measured with a 100- $\Omega$  platinum resistance thermometer (ISOTECH 909/100) with an uncertainty estimated to be  $\pm 0.02$  K. Pressure was measured by means of a pressure gauge (RUSKA 6000) with a full scale of 3500 kPa. The uncertainty in the pressure measurement was estimated to be within  $\pm 1$  kPa, including the accuracy of the pressure transducer and the stability of the pressure during the measurements. The composition of the vapor and liquid phases was determined by means of a gas chromatograph (Hewlett-Packard 6890) connected in-line to the VLE cell. The response of the FID detector was carefully calibrated using gravimetrically prepared mixtures. Considering the reproducibility of the gas chromatograph, the stability of the composition during the measurements, and the uncertainty in calibration, we estimated the uncertainty in composition measurements to be within  $\pm 0.003$  in mole fraction for the liquid and vapor phases.

## Results

The  $T$ – $P$ – $x$ – $y$  data were measured at three isotherms between (263.15 and 293.15) K, and the experimental data are presented in Table 1. Present and literature VLE data<sup>6</sup> are shown in Figure 1. For two points at 263.15 K, the liquid-phase composition was not measured because some problems appeared in the sampling of the mixtures for the analysis. This system shows a strong positive deviation from Raoult's law with the presence of an azeotrope. In the experimental temperature range, the liquid phase is homogeneous, and this behavior is in good agreement with our mutual solubility data<sup>1</sup> measured between 220 and 246 K in the presence of a vapor phase in equilibrium with the liquid phases. The upper critical end point (UCEP) at  $T = 246$  K was found.<sup>1</sup> For a better illustration of the system

\* To whom correspondence should be addressed. E-mail: laura.fedele@ite.cnr.it. Tel: +39 049 8295706. Fax +39 049 8295728.

<sup>†</sup> Institute of Building Technologies.

<sup>‡</sup> Polish Academy of Sciences.

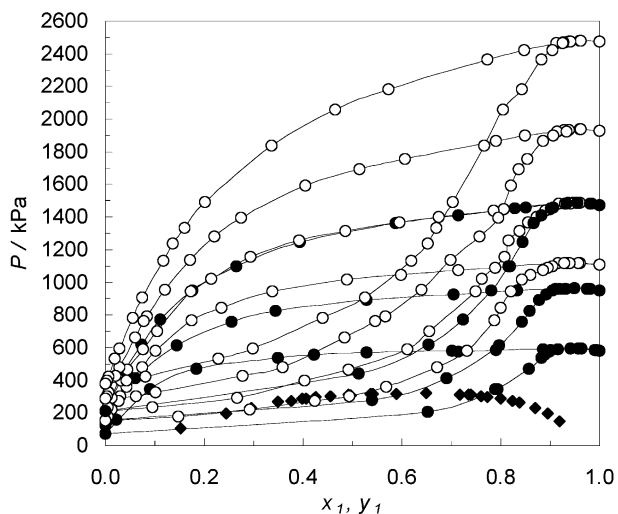


**Figure 1.** Vapor–liquid equilibria data for the R32 (1) + R600 (2) system: ●, present data; ○, Shimawaki and Fujii,<sup>6</sup> —, course of the VLE boundary; ◆, mutual solubility data.<sup>1</sup>

**Table 1. Experimental Vapor–Liquid Equilibria Data for the R32 (1) + R600 (2) System**

$T = 263.15$ K			$T = 278.15$			$T = 293.15$ K		
$x_1$	$y_1$	$P/\text{kPa}$	$x_1$	$y_1$	$P/\text{kPa}$	$x_1$	$y_1$	$P/\text{kPa}$
0.0000	0.0000	69.6	0.0000	0.0000	125.1	0.0000	0.0000	209.4
	0.6520	207.3	0.0267	0.5400	278.5	0.0353	0.5124	441.0
	0.7895	345.1	0.0609	0.6903	410.8	0.0730	0.6546	619.0
0.0903	0.7936	346.3	0.1452	0.7969	614.8	0.1114	0.7232	770.9
0.1847	0.8579	468.4	0.2553	0.8424	760.1	0.1766	0.7803	951.6
0.3499	0.8821	539.2	0.3451	0.8594	826.6	0.2649	0.8153	1098.1
0.4223	0.8883	556.6	0.5287	0.8779	893.7	0.3942	0.8445	1246.0
0.5286	0.8906	568.7	0.7045	0.8914	927.9	0.5867	0.8674	1360.4
0.7009	0.8967	579.0	0.8340	0.9054	948.3	0.7149	0.8822	1412.5
0.7144	0.8979	574.8	0.9115	0.9302	960.4	0.8286	0.9016	1452.7
0.7909	0.9022	585.6	0.9197	0.9311	961.2	0.8509	0.9070	1460.2
0.8858	0.9164	591.7	0.9496	0.9497	963.0	0.9174	0.9326	1480.2
0.9409	0.9407	593.8	0.9803	0.9753	961.2	0.9526	0.9559	1484.8
0.9643	0.9565	592.5	1.0000	1.0000	949.6	0.9844	0.9817	1480.8
0.9931	0.9898	585.4				1.0000	1.0000	1473.2
1.0000	1.0000	580.2						

behavior, the solubility data for the R32 + R600 system, already presented,<sup>1</sup> are also included in Figure 1. The composition of the azeotrope at each temperature was calculated by finding a maximum on the bubble-point curve; at that point, the composition of the vapor and liquid phases is equal. The azeotropic compositions that we found are slightly temperature-dependent with an average value around  $x_{R32} = 0.95$  that increases with rising temperature. This value is close to experimental values reported by Shimawaki and Fujii<sup>6</sup>, even if these data are clearly more scattered and have a less evident temperature trend. The results are shown in Table 2 and in Figure 2, where the published azeotropic compositions,<sup>6</sup> both experimental and calculated, are also included.

To check the data consistency, the vapor pressures of pure R32 and R600 were compared with data calculated by REFPROP 7.0.<sup>8</sup> As shown by Table 3, these data are in good agreement, and the deviations are within the experimental uncertainty.

### VLE Data Correlation

First, the Carnahan–Starling–De Santis (CSD)<sup>9</sup> equation of state (EoS) was applied along with the classical mixing rules. In this equation, both  $a$  and  $b$  parameters

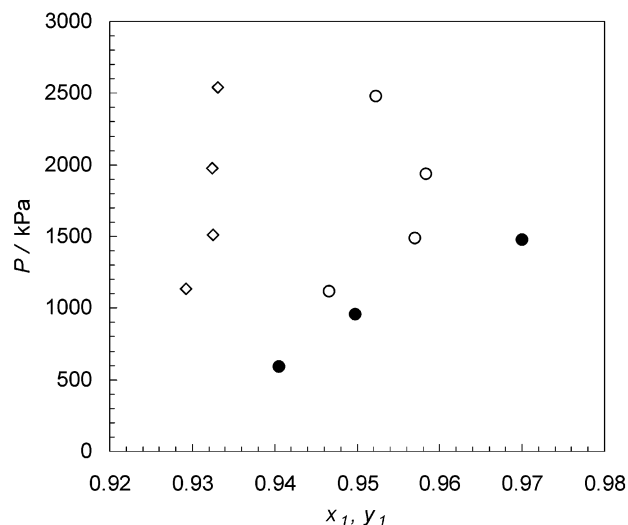


**Figure 2.** Azeotropic data for the R32 (1) + R600 (2) system: ●, this work at 263.15, 278.15 and 293.15 K; ○, reported as experimental; ◇, calculated by Shimawaki and Fujii<sup>6</sup> at 283.15, 293.15, 303.15, and 313.15 K.

**Table 2. Azeotropic Composition and Pressures for the R32 (1) + R600 (2) System**

$T/\text{K}$	$x_{1,\text{azeo}}$	$P_{\text{azeo}}/\text{kPa}$
Present Data		
263.15	0.941	591
278.15	0.950	960
293.15	0.971	1480
Shimawaki and Fujii's Data <sup>6</sup> (Exptl)		
283.15	0.9466	1119
293.15	0.9570	1487
303.15	0.9583	1938
313.15	0.9523	2482
Shimawaki and Fujii's Data <sup>6</sup> (Calcd)		
283.15	0.9292	1135
293.15	0.9325	1511
303.15	0.9324	1976
313.15	0.9331	2542

**Table 3. Comparison between the Present R32 and R600 Vapor Pressure Data and Those Calculated by REFPROP 7.0<sup>8</sup>**

$T/\text{K}$	$P_{\text{exptl}}/\text{kPa}$	$P_{\text{REFPROP 7.0}}/\text{kPa}$	$\Delta P^a/\text{kPa}$	$\Delta P\%^b$
R32				
263.15	580.2	582.6	-2.4	-0.41
278.15	949.6	951.5	-1.8	-0.19
293.15	1473.2	1474.6	-1.4	-0.09
R600				
263.15	69.6	69.8	-0.2	-0.24
278.15	125.1	124.5	0.6	0.45
293.15	209.4	208.0	1.4	0.67

$$^a \Delta P = P_{\text{exptl}} - P_{\text{calcd}}, \quad ^b \Delta P\% = 100 \left( \frac{P_{\text{exptl}} - P_{\text{calcd}}}{P_{\text{calcd}}} \right)$$

are temperature-dependent, and the related expressions along with their coefficients were implemented from REFPROP 5.0.<sup>10</sup> The results of this correlation are summarized in Table 4. The  $k_{ij}$  parameters obtained by fitting are shown in Table 5. Analyzing the deviations in both pressure and vapor-phase composition, we find that the CSD EoS proves to be unable to describe the system, showing very high deviations with an S-shaped distribution if plotted against the liquid-phase composition.

To improve the data correlation, as a second step, the Redlich–Kwong–Soave (RKS)<sup>11</sup> and the Peng–Robinson (PR)<sup>12</sup> EoS's were considered, together with the Huron–

**Table 4. Results of the VLE Data Representation for the R32 (1) + R600 (2) System with Different Models**

T/K	AAD		bias	
	$\Delta y^3$	$\Delta P\%$	$\Delta y^3$	$\Delta P\%$
CSD EoS				
263.15	0.0182	7.03	0.0084	-1.75
278.15	0.0304	8.10	0.0255	-1.05
293.15	0.0231	7.36	0.0207	-1.35
RKS-HV-NRTL ( $\alpha = 0.34$ )				
263.15	0.0045	0.31	0.0040	-0.07
278.15	0.0051	0.84	0.0049	0.18
293.15	0.0059	0.49	0.0059	0.09
PR-HV-NRTL ( $\alpha = 0.34$ )				
263.15	0.0048	0.32	0.0044	-0.08
278.15	0.0055	0.84	0.0055	0.18
293.15	0.0069	0.49	0.0069	0.09
RKS-WS-NRTL ( $\alpha = 0.3$ )				
263.15	0.0052	0.23	0.0050	-0.08
278.15	0.0074	0.76	0.0074	0.40
293.15	0.0062	0.42	0.0061	0.10
LJ Model (Fit Parameters)				
263.15	0.0056	1.07	0.0028	-0.18
278.15	0.0088	2.05	0.0059	1.31
293.15	0.0077	1.63	0.0059	1.56

**Table 5. Regressed Parameters for the Different Models Used in the VLE Data Correlation for the R32 (1) + R600 (2) System**

CSD EoS					
T/K	$k_{ij}$				
263.15	0.15213				
278.15	0.17084				
293.15	0.17918				
RKS-HV-NRTL ( $\alpha = 0.34$ )					
T/K	$\Delta g_{12}$	$\Delta g_{12}$			
263.15	5737.26	3553.86			
278.15	5310.78	3371.50			
293.15	5257.26	3026.02			
PR-HV-NRTL ( $\alpha = 0.34$ )					
T/K	$\Delta g_{12}$	$\Delta g_{12}$			
263.15	5709.65	3557.74			
278.15	5283.94	3381.21			
293.15	5229.24	3041.86			
RKS-WS-NRTL ( $\alpha = 0.3$ )					
T/K	$k_{12}$	$\Delta g_{12}$	$\Delta g_{12}$		
263.15	0.24	5937.00	3766.64		
278.15	0.22	6084.20	3774.46		
293.15	0.32	4596.18	3198.57		
LJ Model (Fit Parameters)					
T/K	$k_t$	$k_v$	$F_{pq}$	$\beta$	$\gamma$
263.15	0.8240	0.9207	1.7743	0.8919	1.0796
278.15					
293.15					

Vidal<sup>13</sup> (HV) mixing rule. In the HV mixing rule, the EoS  $a$  and  $b$  parameters take the form

$$a = b \left[ \sum_{i=1}^n x_i \frac{a_{ii}}{b_{ii}} - \frac{g_{\infty}^E}{C} \right] \quad (1)$$

$$b = \sum_{i=1}^n x_i b_{ii} \quad (2)$$

where  $C$  is an EoS specific constant. For the RKS EoS,  $C = \ln(2)$ , and for the PR EoS,  $C = 0.632252$ .

In both cases, the NRTL<sup>14</sup> equation was used for the excess Gibbs energy representation at infinite pressures in the form

$$\frac{g^E}{RT} = x_1 x_2 \left[ \frac{\tau_{21} G_{21}}{x_1 + x_2 G_{21}} + \frac{\tau_{12} G_{12}}{x_2 + x_1 G_{12}} \right] \quad (3)$$

where  $\tau_{ij}$  and  $G_{ij}$  are equation parameters defined by

$$\tau_{12} = \frac{\Delta g_{12}}{RT} \quad \tau_{21} = \frac{\Delta g_{21}}{RT}$$

$$G_{12} = \exp(-\alpha \tau_{12}) \quad G_{21} = \exp(-\alpha \tau_{21}) \quad (4)$$

and  $\Delta g_{ij}$  and  $\alpha$  can be regressed on the experimental data.

Here in the NRTL equation, the  $\alpha$  parameter was considered to be the third adjustable parameter, varying between 0.30 and 0.38. Both are cubic equations of state giving similar deviations from the experimental data. For both models (i.e., the RKS-HV-NRTL and the PR-HV-NRTL), the best results are achieved using  $\alpha = 0.34$  and they are reported in Table 4, whereas the regressed parameters are collected in Table 5. This model well correlates all of the experimental data, giving deviations well within the estimated measurements' uncertainty.

Moreover, the two cubic equations of state were used to correlate the VLE data using the Wong-Sandler (WS)<sup>15,16</sup> mixing rule in the form

$$a = b \left[ \sum x_i \frac{a_i}{b_i} + \frac{a_{\infty}^E}{C} \right] \quad (5)$$

$$b = \frac{\sum \sum x_i x_j \left( b - \frac{a}{RT} \right)_{ij}}{1 + \frac{a_{\infty}^E}{RT} - \sum x_i \left( \frac{a_i}{b_i RT} \right)} \quad (6)$$

where  $a_{\infty}^E$  is the excess Helmholtz energy at infinite pressure,  $C$  is a constant (defined above), and

$$\left( b - \frac{a}{RT} \right)_{ij} = \frac{(1 - k_{ij})}{2} \left[ \left( b_i - \frac{a_i}{RT} \right) + \left( b_j - \frac{a_j}{RT} \right) \right] \quad (7)$$

The NRTL equation was used to represent  $a_{\infty}^E$  at infinite pressures, again, but fixing  $\alpha = 0.3$ .

Both of these models give similar results and only those related to the RKS-WS-NRTL are shown in Table 4, whereas the regressed parameters are given in Table 5.

As a further step, the Lemmon-Jacobsen (LJ)<sup>17</sup> Helmholtz energy model was applied. In the LJ model, the excess Helmholtz energy takes the form

$$a^E = \sum_{p=1}^r \sum_{q=p+1}^r F_{pq} \sum_{k=1}^{10} N_k \delta_m^{i_k} \tau_m^{i_k} \quad (8)$$

Equation 8 is a function of 10 coefficients, and the mixture reduced temperature and density are determined from

$$\tau_m = \frac{T_{c,m}}{T} \quad \text{and} \quad \delta_m = \frac{\rho}{\rho_{c,m}} \quad (9)$$

**Table 6. Results of the VLE Data Representation with the PR–WS–NRTL Model for the Present Data and Published Data<sup>6</sup> for the R32 (1) + R600 (2) System**

$T/K$	$k_{12}$	$\Delta g_{12}$	$\Delta g_{21}$	AAD( $\Delta P\%$ )	AAD( $\Delta y$ )
Shimawaki and Fujii <sup>6</sup>					
283.15	0.3378	5088.9	2804.2	1.932	
293.15	0.3450	5054.5	2727.7	1.843	
303.15	0.3436	5227.7	2763.7	1.928	
313.15	0.3368	5498.0	2765.6	2.357	
Present Regression of the Shimawaki and Fujii <sup>6</sup> VLE Data					
283.15	0.31	4776.90	2970.32	0.88	0.0133
293.15	0.33	4439.96	2786.71	0.71	0.0177
303.15	0.37	3593.06	2772.43	0.17	0.0233
313.15	0.31	4930.42	2612.87	0.43	0.0192
This Work					
263.15	0.23	5835.56	3743.12	0.23	0.0055
278.15	0.24	5577.53	3623.01	0.76	0.0072
293.15	0.29	4824.63	3203.57	0.42	0.0077

where  $T_{c,m}$  and  $\rho_{c,m}$  are pseudocritical mixture parameters, estimated by means of the nonlinear mixing rules

$$T_{c,m} = \sum_{i=1}^n x_i T_{c,i} + \sum_{i=1}^{n-1} \sum_{j=i+1}^n x_i^\beta x_j^\psi (k_t - 1) \quad (10)$$

$$\rho_{c,m} = \left[ \sum_{i=1}^n \frac{x_i}{\rho_{c,i}} + \sum_{i=1}^{n-1} \sum_{j=i+1}^n x_i x_j (k_v - 1) \right]^{-1} \quad (11)$$

The five interaction parameters of the model ( $k_t$ ,  $k_v$ ,  $F_{pq}$ ,  $\beta$ , and  $\psi$ ) were regressed to describe the system and were kept constant over the considered temperature range. The results are also shown in Table 4, and the regressed parameters are summarized in Table 5. This model is able to describe the experimental data quite well but gives clearly greater deviations from the fit at lower mole fractions of R32.

Finally, these data were compared with the database REFPROP 7.0.<sup>8</sup> For the R32 + R600 system, this database uses the LJ model based on estimated interaction parameters because no experimental data were available to regress the model. The deviations between the experimental data and REFPROP 7.0 are AAD( $\Delta P\%$ ) = 11.05% and AAD( $\Delta y$ ) = 0.0167. It is evident that the software is unable to predict the saturation boundaries of this system adequately.

### Comparison with Literature Data

On the basis of the model used by Shimawaki and Fujii<sup>6</sup> for the correlation of the VLE data of this strongly nonideal system, a comparison between the published data<sup>6</sup> and those presented here was made. The Peng–Robinson equation of state with the Wong–Sandler mixing rules was applied by correlating the VLE data for each source and isotherm individually. In Table 6, the results of the correlation are summarized, also including the reported values in the Shimawaki and Fujii paper.<sup>6</sup> The difference in the resulting parameters from the two independent correlations of the Shimawaki and Fujii<sup>6</sup> data is interesting, even if the employed model is the same. Presumably it is due to the regression software that was used and the conditions imposed for the convergence. Moreover, the present correlation gives smaller deviations in terms of saturated pressure than those reported in ref 6. In addition, as shown in Figure 3, the present correlation gives random and similar pressure deviations for data from both sources. On the contrary, the deviations in terms of vapor-phase composition, presented in Figures 4, are of opposite sign

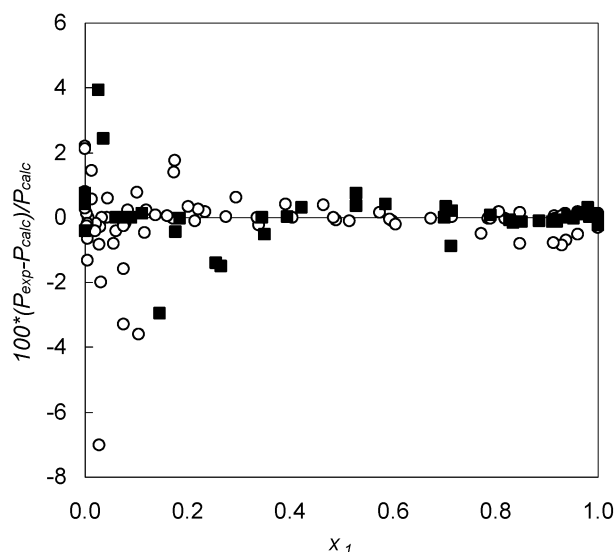


**Figure 3.** Saturation pressure deviations from the PR–WS–NRTL model: ■, data presented here; ○, data reported by Shimawaki and Fujii.<sup>6</sup>

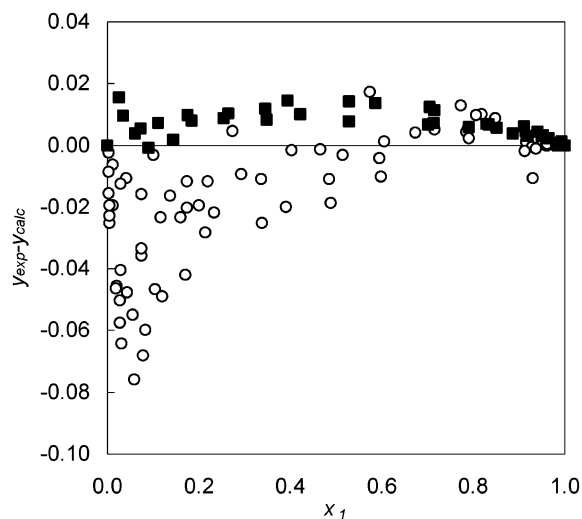


**Figure 4.** Vapor-phase composition deviations from the PR–WS–NRTL model: ■, data presented here; ○, data taken from Shimawaki and Fujii.<sup>6</sup>

from the two sources and are significantly smaller for the present results.

### Conclusions

Forty-five vapor–liquid equilibria experimental data points were measured at 263.15, 278.15, and 293.15 K. The R32 + R600 system shows a strong positive deviation from Raoult's law, with the presence of an azeotrope at  $x_{R32} = 0.95$  in mole fraction.

Few models were considered to represent the system behavior. The CSD EoS, together with the classical mixing rule, was not demonstrated to correlate the experimental data successfully. Better agreement with the data was found with the RKS and the PR EoS, together with the Huron–Vidal and/or the Wong–Sandler mixing rules, using the NRTL equation to represent the excess Gibbs energy. The LJ model was applied, both in the correlative and in the predictive mode (i.e., the REFPROP 7.0 database). The LJ model proved to work successfully in the correlative mode, representing the experimental data with AAD( $\Delta P\%$ ) = 1.58% and an AAD( $\Delta y$ ) = 0.0074. On the

contrary, it is not able to represent the VLE data well if used in a predictive mode, as in the database REFPROP 7.0 with  $AAD(\Delta P\%) = 11.05\%$  and  $AAD(\Delta y) = 0.0167$ .

A comparison with the available literature data was done on the basis of the correlation of these data with the PR-WS-NRTL model. It proved that this set of data and the Shimawaki and Fujii<sup>6</sup> data are consistent in terms of saturated pressure but not in terms of vapor-phase composition, with absolute average deviations between the data and the model of  $AAD(\Delta P\%) = 0.55\%$  and  $AAD(\Delta y) = 0.0184$  for the Shimawaki and Fujii<sup>6</sup> data and  $AAD(\Delta P\%) = 0.47$  and  $AAD(\Delta y) = 0.0068$  for the present data.

### Acknowledgment

R.S. is indebted to the CNR-ITC in Padova for the financial support of his visit. We are grateful to Professor Fabio Polonara for his kind help.

### Literature Cited

- (1) Bobbo, S.; Fedele, L.; Camporese, R.; Stryjek, R. VLLE measurements and their correlation for the R32 + R600 system. *Fluid Phase Equilib.* **2003**, *210*, 45–56.
- (2) Bobbo, S.; Fedele, L.; Camporese, R.; Scattolini, M.; Stryjek, R. Mutual solubility and VLLE correlation for the R32 + R290 system. *Fluid Phase Equilib.* **2003**, *212*, 245–255.
- (3) Fedele, L.; Bobbo, S.; Camporese, R.; Stryjek, R. *Fluid Phase Equilib.* **2004**, *222–223*, 283–289.
- (4) Bobbo, S.; Fedele, L.; Camporese, R.; Stryjek, R. VLE measurements and modeling for the strongly positive azeotropic R32 + propane system. *Fluid Phase Equilib.* **2002**, *199*, 175–183.
- (5) Fedele, L.; Bobbo, S.; Camporese, R.; Stryjek, R. To be submitted for publication.
- (6) Shimawaki S.; Fujii K. Vapor-Liquid Equilibria of HFC-32/n-Butane Mixtures. *Int. J. Thermodyn.* **2003**, *24*, 1033–1042.
- (7) Bobbo, S.; Stryjek, R.; Elvassore, N.; Bertucco, A. A recirculation apparatus for vapor-liquid equilibrium measurements of refrigerants. Binary mixtures of R600a, R134a and R236fa. *Fluid Phase Equilib.* **1998**, *150–151*, 343–352.
- (8) Lemmon, E. W.; McLinden, M. O.; Huber, M. L. *NIST Reference Fluid Thermodynamic and Transport Properties (REFPROP)*, version 7.0; Physical and Chemical Properties Division, National Institute of Standards and Technology: Gaithersburg, MD, 2002.
- (9) De Santis, R.; Gironi, F.; Marrelli, L. Vapor-liquid equilibrium from a hard sphere equation of state. *Ind. Eng. Chem. Fundam.* **1976**, *15*, 183–189.
- (10) Huber, M.; Gallagher, J.; McLinden, M.; Morrison G. *NIST Thermodynamic Properties of Refrigerants and Refrigerant Mixtures Database (REFPROP)*, version 5.0; Thermophysics Division, National Institute of Standards and Technology: Gaithersburg, MD, 1996.
- (11) Soave, G. Equilibrium constants from a modified Redlich-Kwong equation of state. *Chem. Eng. Sci.* **1972**, *27*, 1197–1203.
- (12) Peng, D. Y.; Robinson, D. B. A New Two-Constant Equation of State. *Ind. Eng. Chem. Fundam.* **1976**, *15*, 59–64.
- (13) Huron, M. J.; Vidal, J. New Mixing Rules in Simple Equations of State for Representing Vapor-Liquid Equilibria of Strongly Non-Ideal Mixtures. *Fluid Phase Equilib.* **1979**, *3*, 255–272.
- (14) Renon, H.; Prausnitz, J. M. Local Compositions in Thermodynamic Excess Functions for Liquid Mixtures. *AIChE J.* **1968**, *14*, 135–144.
- (15) Wong, D. S. H.; Sandler S. I. A Theoretically Correct Mixing Rule for Cubic Equations of State. *AIChE J.* **1992**, *38*, 671–680.
- (16) Wong D. S. H.; Orbey H.; Sandler S. I. Equation of State Mixing Rule for Nonideal Mixtures using Available Activity Coefficient Model Parameters and that Allows Extrapolation over Large Ranges of Temperature or Pressure. *Ind. Eng. Chem. Res.* **1992**, *31*, 2033–2039.
- (17) Lemmon, E. W.; Tillner-Roth, R. A Helmholtz energy equation of state for calculating the thermodynamic properties of fluid mixtures. *Fluid Phase Equilib.* **1999**, *165*, 1–21.

Received for review March 30, 2004. Accepted September 20, 2004.

JE049874H